

Intrazeolite Photochemistry. 12. Ship-in-a-Bottle Synthesis and Control of the Photophysical Properties of 9-(4-Methoxyphenyl)xanthenium Ion Imprisoned into Large-Pore Zeolites

María Luz Cano,[†] Frances L. Cozens,^{*,‡} Vicente Fornés,[†] Hermenegildo García,^{*,†} and J. C. Scaiano[‡]

Instituto de Tecnología Química CSIC-UPV, Universidad Politécnica de Valencia, 46071 Valencia, Spain, and Department of Chemistry, University of Ottawa, Ottawa, Canada, K1N 6N5

Received: March 8, 1996; In Final Form: August 2, 1996[⊗]

The 9-(4-methoxyphenyl)xanthylium ion (AnX^+), a bulky cation that according to molecular modeling simulations cannot enter through the 7.4 Å pore opening of tridirectional large-pore zeolites Y and β , has been prepared by ship-in-a-bottle synthesis within the supercages of these two zeolites. The synthetic procedure involves two steps: (i) generation of xanthylium cation (X^+) adsorbed within the zeolite by treatment of xanthrol onto the H^+ form of these solids; (ii) electrophilic attack of the cation to anisole within the framework of the zeolite. Carrying out the same procedure using toluene or benzene or using an alternative process involving the reaction of xanthone with anisole, led to the corresponding 9-arylxanthylium ions together with some unidentified adventitious material. Textural and acidic properties of these composites were tested using α -methylstyrene dimerization and were found to be very similar to the original HY or H β zeolites, thus indicating an internal location for AnX^+ . Entrapment within the zeolite framework restricts AnX^+ conformational mobility, thwarting the deactivation pathway occurring in solution. This has allowed for the first time characterization of its triplet excited state as a long-lived transient species (tens of microseconds), as well as the observation of room-temperature fluorescence in the nanosecond range.

Introduction

Zeolites have proved to be very convenient hosts to study the photophysical and photochemical properties of persistent, adsorbed organic cations.^{1–5} Stabilization of these reaction intermediates arises not only from the internal electrostatic fields occurring inside the voids of these microporous solids^{6–8} but also in many cases from the tight fit of the rigid, inert framework that protects these cations from the attack of nucleophilic species, and in particular from physisorbed water. Thus, we have previously observed that samples of xanthylium ions (X^+) included within mordenite or ZSM-5 can be stored for a period of years without any noticeable alteration of their spectroscopic properties.² However, despite these very promising properties, the number of studies dealing with the use of zeolites as a solid matrix is still very small and much work remains to be done in this area. To further expand the type of cations that can be incorporated, the preparation and characterization of bulky organic cations (those whose smallest cross section is larger than 7.4 Å) inside the cages of large-pore zeolites is particularly challenging. This is due to the special geometry of tridirectional zeolites such as Y and β , that, despite having cages and cavities of large dimensions (about 13 Å), are accessible only through much smaller round pore openings, (typically around 7.4 Å) that severely limit the size of the species able to gain access to these cages.

Zeolites are crystalline aluminosilicates whose crystalline structure is formed by channels and cavities of strictly regular dimensions called micropores. According to the dimensions of these internal voids, zeolites have been classified as small, medium, and large pore, when their pore apertures are formed by rings containing 8, 10, or 12 oxygen atoms, respectively.⁹

These intracrystalline voids of zeolites are accessible to guest molecules whose molecular sizes are smaller than the apertures of the pores. The ability of zeolites to incorporate guest species gives rise to a supramolecular chemistry and several terms such as molecular sieves,⁷ microscopic reactors,¹⁰ molecular pockets,¹¹ or reaction cavities¹² have been coined to describe the porosity of zeolites at a molecular level. Up to six years ago, it was a clear limitation in the size of a molecule that could be hosted in zeolites. However, more recently has been reported a novel family of extra-large-pore aluminosilicates,¹³ generally referred to as mesoporous materials to distinguish from classical microporous zeolites. Thus, MCM-41 is formed by an array of parallel hexagonal channels whose diameter can be controlled from 20 to 60 Å by varying the chain length of the surfactant used as template during its synthesis.¹⁴

Apart from the dimensions of the micropores, the geometry of the internal voids is another important factor to be considered since it determines the diffusion coefficient of the guest and, related to this, the uptake that can be incorporated in the internal surfaces. In this respect, zeolites can be classified as monodirectional (system of parallel channels), bidirectional (two system of channels crossing), or tridirectional (system of cages interconnected).

In the present series of articles, we have employed zeolites of medium-, large-, and extra-large-pore size as well as mono-, bi-, and tridirectional topologies to control and modify the photochemical properties of embedded organic species. The structure of some representative zeolites is illustrated in Chart 1. Our systems provides new examples of the potential of zeolites as rigid matrixes to stabilize and immobilize organic species.

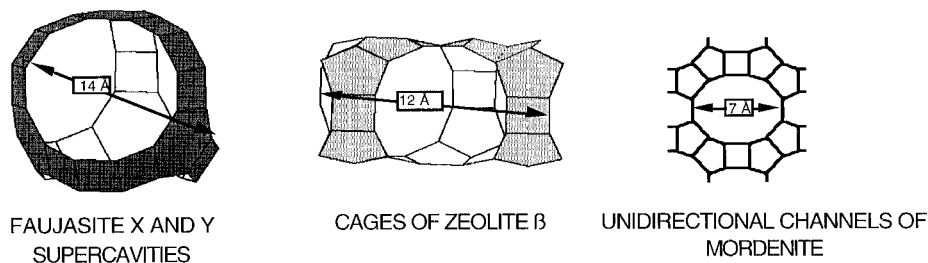
Ship-in-a-bottle methodologies have to be devised to synthesize large cations that afterward will remain imprisoned inside the zeolite supercages.^{1,3,15–17} This methodology has sometimes failed in the past to produce well-defined species entrapped

[†] Universidad Politécnica de Valencia.

[‡] University of Ottawa.

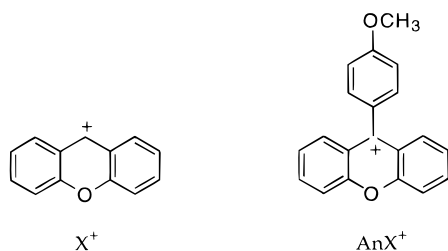
[⊗] Abstract published in *Advance ACS Abstracts*, October 15, 1996.

CHART 1



inside the voids of large-pore zeolites,^{18–21} and therefore a careful characterization of the resulting zeolite-bound organic species is necessary in order to establish their purity and the absence of adventitious material. We have already successfully reported the synthesis of the 2,4,6-triphenylpyrylium cation encapsulated within zeolite Y by emulating homogeneous phase procedures.¹ In the present work, we take advantage of the extraordinary ability of the zeolite to spontaneously generate and stabilize positively charged species from neutral precursors to prepare the 9-(4-methoxyphenyl)xanthylium ion (AnX^+) inside the micropores of zeolites Y and β . The presence of AnX^+ as the sole species, together with the absence of detectable amounts of X^+ was ascertained by IR spectroscopy of the resulting samples. To the best of our knowledge, the procedure that was carried out to generate the cation within the zeolite has not been reported in liquid solution.

We have previously studied the photophysical properties of the parent unsubstituted X^+ incorporated within medium- and large-pore zeolites.² Herein, we have found that AnX^+ immobilized inside the zeolite supercages shows photochemical behavior similar to that of X^+ . Thus, besides intense, long-lived fluorescence we have observed a strong band in the visible region for the triplet excited state of the cation, together of an absorption at 340 nm attributed to the corresponding AnX^* radical. These findings sharply contrast with previous studies of AnX^+ in solution which failed to observe any excited state of AnX^+ at room temperature.²²



Results and Discussion

Preparation of the AnX^+ -HZeolite. Molecular modeling predicts that although 9-aryl-substituted xanthylium ions can be accommodated inside the Y supercage, they cannot enter through the 12-member-ring pore opening. A visualization of the optimized conformation of AnX^+ within the supercage of zeolite Y is provided in Figure 1. In fact, it has been previously reported that similarly shaped 9-phenylanthracene cannot enter through the zeolite Y windows.^{23–25}

In addition, we tried to generate the 9-phenylxanthylium ion (PhX^+) by adsorbing $PhXOH$ from a dichloromethane solution onto acid Y zeolite. Although the suspension become yellow in color, it faded completely almost immediately after filtering the solid. The amount of organic material adsorbed on the solid was very low (<0.5%) as determined by combustion chemical analysis and thermogravimetry. Loss of color of the sample combined with the low amount of organic material indicate that

only the external, more exposed surface of the zeolite particles was accessible to $PhXOH$ under these adsorption conditions.

In contrast, an alternative strategy depending on the prior generation of X^+ followed by treatment of the resulting composite at reflux temperature with anisole turned out to be a successful procedure to prepare AnX^+ incorporated inside Y and β zeolites.

First we prepared the less bulky parent X^+ by adsorption of XOH from a dichloromethane solution onto the H^+ -form of zeolites Y and β . The diffuse reflectance and IR spectra of the resulting complexes were coincident with those previously reported for these types of samples.² After the characterization of the solids the zeolites containing X^+ were reacted with neat anisole. The large excess of anisole compared to X^+ , as well as the relatively high reaction temperature ensure that essentially all X^+ is consumed during the synthesis. This was confirmed by IR spectroscopy (vide infra). Once the reaction was complete, the samples were submitted to exhaustive solid–liquid extraction until no more organic material could be recovered from the orange solids. The reaction sequence for the synthesis of AnX^+ is outlined in Scheme 1; the observation (GC-MS) of the formation of minor amounts of a product compatible with $AnXH$ (MW 288) in the supernatant lends support to the proposed mechanism.

Formation of a C–C bond between X^+ and the aromatic ring of anisole can be easily rationalized as an aromatic electrophilic Friedel–Crafts reaction between X^+ and the electron-rich aromatic compound to give an intermediate cyclohexadienyl cation.²⁶ In addition, attempts to reproduce this treatment using toluene or benzene as the aromatic instead of anisole did not lead with the same efficiency to the formation of the corresponding 9-aryl-substituted xanthylium ion. This was assessed by the impossibility to obtain for these samples a defined IR spectrum corresponding to these cations embedded in the zeolite matrix. However, the formation of 9-phenyl and 9-*p*-tolylxanthyliums in some extent did occur since the characteristic long wavelength absorption around 500-nm was observed as a low-intensity broad band in the diffuse reflectance spectra of these samples. This is in agreement with the decreasing stability of the intermediate cyclohexadienyl cation upon changing the aryl substituent from 4-MeO to 4-Me or 4-H. Once formed, the cyclohexadienyl cation will deprotonate to generate $AnXH$ within the zeolite framework.

Much less documented is the nature of the proposed hydride abstraction from $AnXH$ which leads to the formation of the organic AnX^+ (Scheme 1). However, we have previously reported that the hydride abstraction yielding X^+ occurs spontaneously by adsorption of the corresponding XH into acid zeolites.²⁷ Furthermore, this phenomenon, although still poorly understood, appears to be general since other carbenium ions can also be generated from their hydrocarbons.^{28,29}

Characterization of the resulting zeolite samples containing AnX^+ was accomplished by combustion chemical analysis, thermogravimetric-differential scanning calorimetry (TG-DSC),

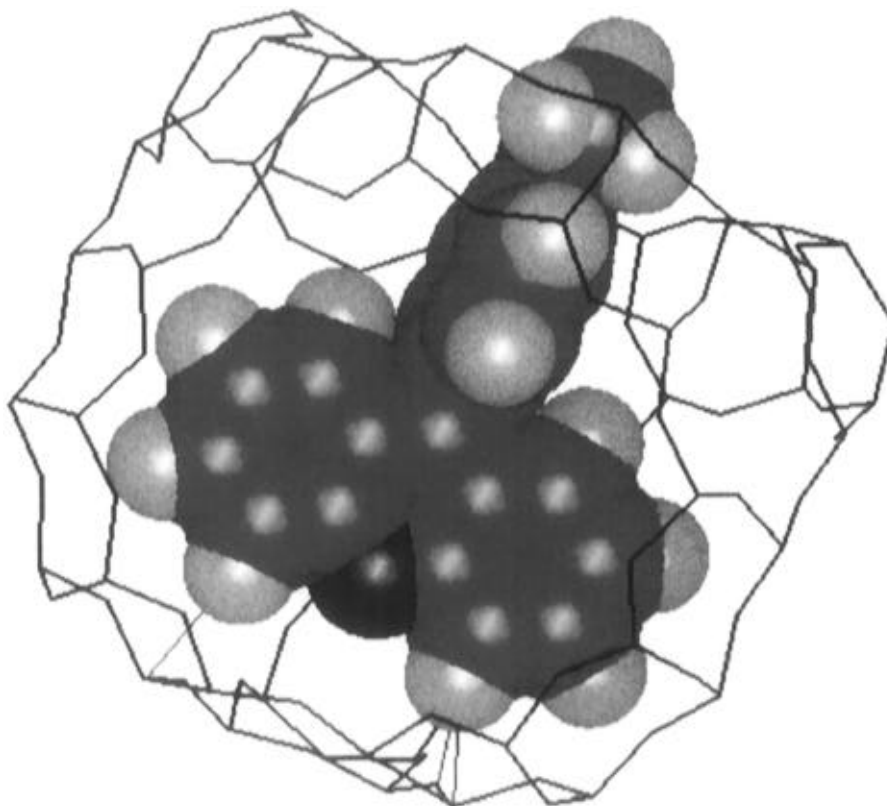


Figure 1. Molecular modeling visualization of AnX^+ cation inside zeolite Y supercage. Docking was performed to minimize overlapping of host–guest atoms. The view is taken through one of the four windows facing the xanthylium core, while the MeO group can be seen partially penetrating through another opening.

SCHEME 1

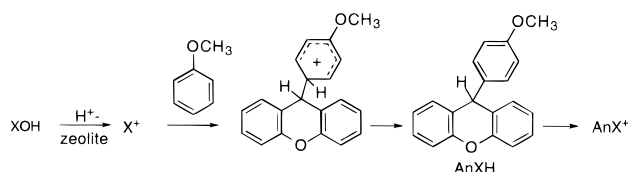


TABLE 1: Some Relevant Physicochemical Parameters of the Samples Containing AnX^+ Cation Incorporated within Zeolites

	$\text{AnX}^+\text{-HY}$	$\text{AnX}^+\text{-H}\beta$	$\text{AnX}^+\text{-MCM-41}$
zeolite Si/Al ratio ^a	2.6	13.0	11.3
BET surface area ($\text{m}^2 \text{g}^{-1}$) ^b	720	666	928
amount of organic material (mg g^{-1} zeolite) ^c	39	36	54
UV/vis absorption bands (nm)	371, 515	370, 495	365, 497
carbon content (%) ^d	2.51	2.49	3.74

^a Measured by atomic absorption spectroscopy after HF disgregation.

^b For the original zeolite prior to the adsorption procedure; calculated according to the algorithm proposed by (BET): Brunauer, S.; Emmett, P. H.; Teller, E. *J. Am. Chem. Soc.* **1938**, *60*, 309. ^c Measured by the loss of weight between 300 and 700 °C in the TG profiles. ^d Determined by combustion chemical analysis.

diffuse reflectance (DR), and IR spectroscopy. Identity of AnX^+ chemical structure and purity was confirmed by comparison with an authentic sample prepared by adsorbing AnXOH onto extra large pore MCM-41^{13,14,30,31} (array of parallel hexagonal channels, 20 Å diameter), where geometrical restrictions do not apply. Some of the relevant physicochemical parameters of the samples that have been prepared are given in Table 1.

The amount of organic material (between 3 and 6 wt %) adsorbed by the solid was determined by combustion elemental analysis of carbon. Alternatively, the AnX^+ content of the

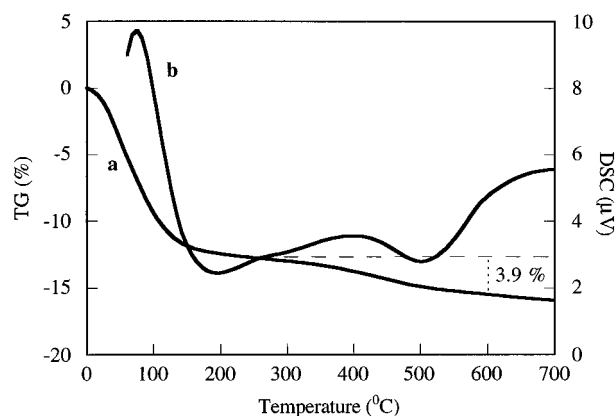


Figure 2. Thermogravimetric profile (a: left axis) and DSC curve (b: right axis) of AnX^+ incorporated within zeolite HY. The loss of weight (3.9%) between 300 and 700 °C corresponds to the exothermic decomposition of organic cation.

zeolite matrixes was obtained from the TG-DSC curves. In this technique the sample is placed in the pan of a microbalance, while it is being progressively heated to 900 °C under air stream. The loss of weight due to the desorption/degradation of the organic material is recorded at each temperature (TG) and simultaneously the absorbed or evolved heat from the sample is measured by comparing to an inert standard of kaolin (DSC). The values obtained by combustion analysis also agree fairly well with the loss of weight observed in the TG curve from 300 to 700 °C, corresponding to an exothermic process peaking at 515 °C (Figure 2). We rationalize this exothermic weight loss as owing to the decomposition of included organic cation.

Diffuse reflectance of these samples exhibited the very characteristic absorption of AnX^+ dye and closely resembled the UV–vis spectrum of AnX^+ in solution. Figure 3 provides a comparison of the UV–vis diffuse reflectance spectra of some

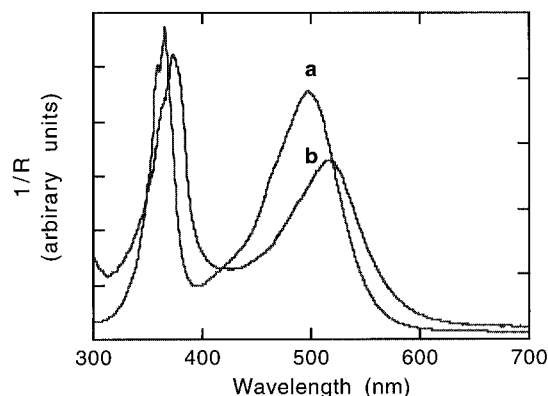


Figure 3. Diffuse reflectance ($1/R$) of the AnX^+ incorporated in MCM-41 by adsorption of AnXOH (plot a) and synthesized in zeolite Y from X^+ (plot b).

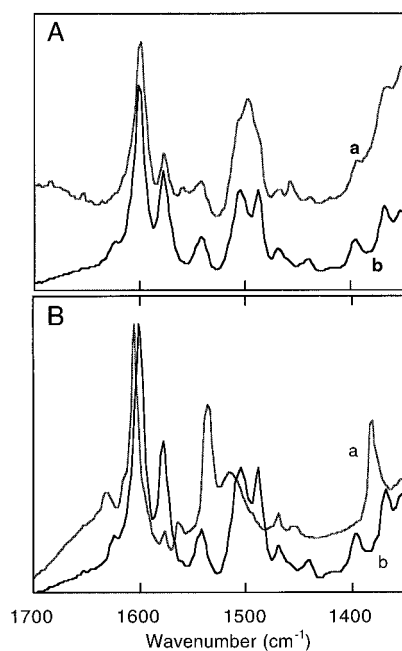
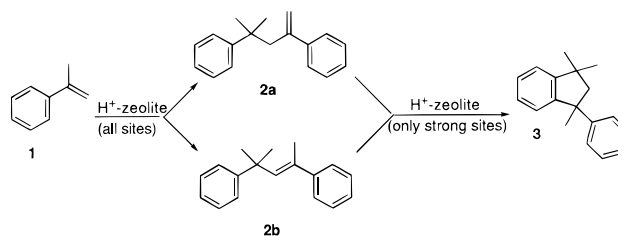


Figure 4. (A) Aromatic region of the FT-IR spectra of AnX-HY (trace a) prepared by ship-in-a-bottle synthesis from xanthylum and AnX-MCM-41 (trace b) obtained by adsorbing AnXOH onto dehydrated MCM-41. Spectra were recorded after outgassing at 200°C under dynamic vacuum (10^{-2} Torr) for 1 h. (B) IR spectra recorded under the same conditions of $\text{X}^+\text{-HMor}$ (trace a) and $\text{AnX}^+\text{-MCM-41}$ (trace b).

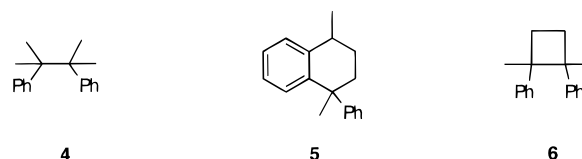
of the samples prepared in this work. These DR spectra, especially the long-wavelength, broad bands, are very different from those corresponding to the precursor X^+ in both solution and zeolite.²

The aromatic region of the IR spectrum of AnX^+ showed many similarities with the parent X^+ when adsorbed on zeolites. However, there are appreciable shifts of the stronger absorption bands, and the appearance of new bands of medium intensity around 1500 cm^{-1} . This is the main piece of evidence to rule out the presence of some residual X^+ . As already mentioned above, a definitive piece of evidence supporting the formation of AnX^+ within zeolites Y and β was the remarkable good match between of the IR spectra of these samples with that obtained after adsorption of AnXOH onto MCM-41 (Figure 4). The background intensity increase at 1350 cm^{-1} and weak broad absorption peaking at 1750 cm^{-1} observed in the spectrum of AnX-HY (trace a in Figure 4A) are characteristic of the HY matrix and are due to the intense Si-O and Al-O stretching bands (1050 cm^{-1}) and lattice overtones. For the sake of

SCHEME 2: Dimer Ratios at Low Conversions: **2a** (9), **2b** (1), **3** (4)



SCHEME 3: Characteristic Dimers Formed Under Radical (4) or Radical Cation (5 and 6) Reaction Mechanisms



comparison, the spectrum of a sample of X^+ adsorbed on zeolite has also been included (Figure 4B).

We attempted an alternative procedure for the preparation of AnX^+ consisting of the treatment of xanthone with anisole in the presence of HY. Although, DR spectra of the samples prepared in this way did show the formation of AnX^+ , IR spectra were complicated by strong absorption bands in addition to those associated with AnX^+ cation. This indicates that some adventitious, unidentified material has also been formed, making these samples inappropriate for their photochemical study.

External versus Internal Location of AnX^+ on the Zeolite Particles. After the ship-in-a-bottle synthesis, the zeolites contain a considerable amount of AnX^+ corresponding to one cation for every two-to-three supercages. We addressed the possibility that a large portion of AnX^+ could be located on the outer surface of the particles and not within the micropores. In heterogeneous catalysis a common, indirect procedure to determine changes in the microporosity of the catalysts owing to the presence of adsorbed, organic material is to use a test reaction to compare the activity of the prepared solid with a fresh sample of the same catalyst.^{32,33}

For this purpose we have chosen the acid-catalyzed dimerization of α -methylstyrene (**1**), which is known to give rise to the olefinic dimers **2** together with the indanic dimer **3** (Scheme 2).³⁴⁻³⁸ Other reaction mechanisms afford different dimers such as **4** or **5** and **6** (Scheme 3).³⁹⁻⁴² Thus, by merely determining the product distribution, it is possible not only to estimate changes in acid strength but also to assess if other reaction mechanisms besides that involving a carbenium ion are intervening.

Therefore, treatment of a solution of **1** in the presence of zeolites containing AnX^+ gave rise to the same product distribution and at very similar initial rate and kinetics than the original samples of zeolites (Scheme 2). This indicates that the textural properties of the zeolites (surface acidity, microporosity) have not been substantially altered during the preparation of AnX^+ . This would not be the case if AnX^+ would have been located on the external surface of the particle, blocking the pores or neutralizing the acid sites.⁴³

It has to be remarked that according to Scheme 1 the actual location of AnX^+ depends to a large extent on the distribution of X^+ before the addition of anisole, since the relocation of the much bulkier AnXH or AnX^+ seems unlikely. In this sense we have already presented experimental evidence supporting

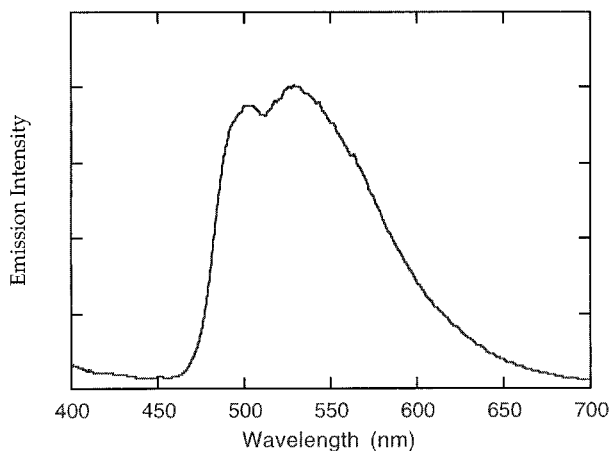


Figure 5. Emission spectra upon 375 nm excitation of AnX⁺ in H β .

the internal location of X⁺ within the micropores of medium and large pore zeolites.²

Photophysical Properties. Xanthylium ions, especially 9-aryl substituted, are among the best studied carbenium ions with regards to their photophysical and photochemical properties.^{44–48} In solution they generally exhibit strong fluorescence (Φ_F between 0.55 and 0.88) with lifetimes from 1 to 50 ns²² while the triplet excited state is characterized by a large extinction coefficient absorption below 300 nm accompanied by a much less intense broad band in the 400–500 nm region and bleaching of ground-state absorption.^{22,49} It has been found that substitution at the 9-position of the tricyclic aromatic rings does not substantially modify this general behavior.⁵⁰ However, AnX⁺ constitutes a remarkable exception in this family. Thus, no fluorescence could be observed at room temperature in solution,²² while the singlet lifetime estimated by indirect measurements at 77 K in a mixture of H₂SO₄/CH₃CN was found to be unusually short (0.14 ns).⁵¹ These anomalies were rationalized assuming a deactivation by intramolecular quenching of the xanthylium moiety by the anisyl substituent occurring in a twisted conformation.²² This type of deactivation pathway requiring conformation mobility can be anticipated to be greatly minimized by entrapment of AnX⁺ within the zeolite supercages and by the anisotropy of the zeolitic host. Thus, perusal of Figure 1 shows AnX⁺ must adopt a more frozen conformation to fit within zeolite supercages. In fact for zeolite Y the methoxy substituent is clearly located in one of the four openings of the cage.

We have been able to observe room-temperature fluorescence from AnX⁺ embedded within zeolites. Figure 5 shows the fluorescence spectra of AnX⁺ in H β after 375-nm excitation. The shape of the spectrum is very similar to that of other xanthylium cations, whereas the confined environment is manifested in the good spectral resolution. The fluorescence lifetime was measured and found to be around 4 ns, which is in the same range as previously reported fluorescence lifetimes for other xanthylium ions in solution. This indicates that the intramolecular quenching of the xanthylium moiety by the anisyl substituent is less effective in the restricted environment provided by the zeolite cage. A similar but weaker emission was also observed for the sample AnX⁺-MCM-41 (prepared by adsorbing AnXOH), although the lifetime was somewhat shorter (\sim 1.3 ns), as expected from the increased freedom of movement in this zeolite. This shows that the thwarting of the nonradiative deactivation pathway is a general phenomenon of the incorporation of AnX⁺ on solid surfaces and rules out the possibility that trace amounts of X⁺ (absent in the AnX⁺-MCM-41 preparation) were responsible for the fluorescence.

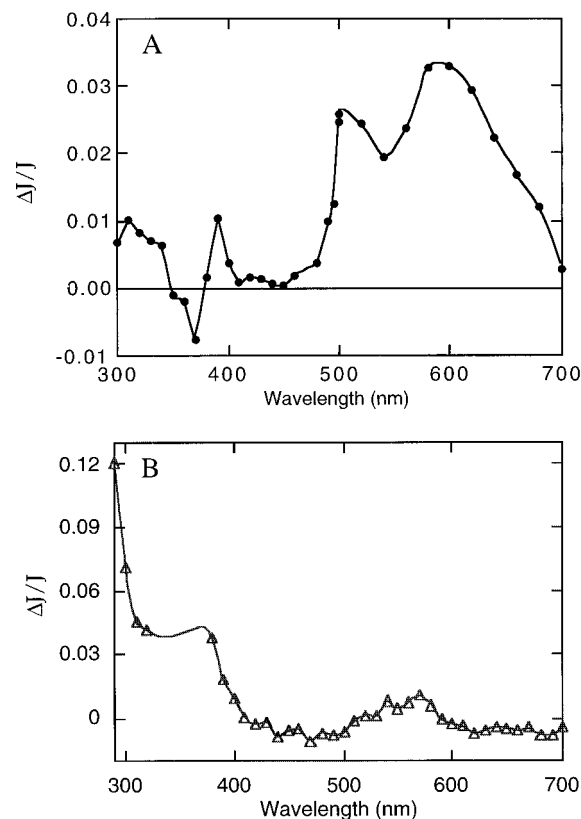


Figure 6. Transient reflectance spectra ($\Delta I/I_0$) recorded 2 μ s after 266 nm excitation of the AnX⁺ in H β (A) and adsorbed in MCM-41 (B).

The transient DR spectra of the AnX⁺ zeolite complexes were found to be very similar to the transient DR spectra of the parent X⁺ incorporated within the zeolite framework.² The characteristic features (Figure 6) include a large band in the visible region (600 nm), corresponding to the triplet excited state of the cation. Along with the 600 nm band the spectra show reflectance at 300 nm which is also attributed to the triplet state of the cation, while bleaching of the cation is observed at 370 nm. The decay of the 300 and 600 nm bands is accompanied with an increase in reflectance at 370 nm due to the recovery of AnX⁺ ground state. This feature, along with appreciable oxygen quenching are consistent with the assignment of the 300 and 600 nm bands to the triplet state of the cation. The 600 nm band is twice as intense as the 300 nm band for AnX⁺-HY and AnX⁺-H β . The transient spectrum of AnX⁺-MCM-41 also exhibits these two absorptions (Figure 6), but in contrast with the samples of AnX⁺ confined in more restricted spaces, the extinction coefficient of the long-wavelength band is weaker than that of the band centered at 300 nm. In fact, the transient spectrum of AnX⁺-MCM-41 is remarkably similar to the T–T absorption spectra for the triplet of many other xanthenium ions in solution.⁴⁹

In addition to the similar triplet spectra, we also observed a small amount of reflectance at 340 nm upon excitation of the cation.² We attribute this reflectance to the AnX^{*} generated by electron transfer from a donor molecule and/or oxygens of the framework to the excited AnX⁺. In solution, AnX^{*} has also been observed during laser flash photolysis work with AnX⁺,²² and the proposed mechanism for its formation was single electron transfer (SET) from adventitious AnXOH to AnX⁺. We think that in our case, a SET from electron-rich oxygens of the framework to excited AnX⁺ is a more likely explanation. Clearly, the unusual photophysical behavior of AnX⁺ has been overcome by entrapment within zeolite cavities.

Conclusions

We have provided spectroscopic evidence showing that AnX^+ can be cleanly prepared by ship-in-a-bottle synthesis from the parent unsubstituted X^+ , through an unprecedented reaction mechanism that relies on the ease of hydride transfer on zeolite surfaces. We have used the dimerization of α -methylstyrene as a test reaction to establish that the textural and acid properties of the zeolites particles are not substantially altered by the preparation procedure or the presence of the organic material, thus supporting that AnX^+ is located within the zeolite supercages.

Incorporation of AnX^+ within the large-pore zeolite framework modifies the photophysical properties of this cation with respect to solution by increasing the fluorescence lifetime at least 30-fold, allowing its measurement at room temperature, as well as to detect for the first time the triplet excited state. This can be reasonably attributed to immobilization of AnX^+ that hinders the deactivation mechanism occurring in solution. These results combined with the ship-in-a-bottle synthesis of AnX^+ nicely show the opportunities that zeolites offer as solid matrixes to control and modify the photochemistry of organic carbenium ions.

Experimental Section

Zeolite HY was prepared starting from a commercial Na^+ form (Union Carbide, SK-40) by three consecutive ion exchange/calcination cycles using aqueous solutions of ammonium acetate following the procedure previously reported.⁵² Zeolite β was prepared by thermal decomposition of an as-synthesized tetraethylammonium sample.⁵³ Mesoporous MCM-41 was obtained from amorphous silica (Aerosil 200, Degussa) using a 25% aqueous mixture of tetraethylammonium hydroxide and hexadecyltrimethylammonium bromide following reported procedures.¹⁴ Pore diameter was measured by Ar adsorption.

9-Xanthidrol, 9-phenylxanthidrol, and xanthone were commercially available (Aldrich) and used as received, while 9-(4-methoxyphenyl)-9-xanthidrol was prepared by Grignard reaction of xanthone with 4-methoxyphenylmagnesium bromide following the procedure previously reported.⁴⁷

Samples containing AnX^+ were prepared by stirring at reflux temperature a mixture of xanthidrol (50 mg) in CH_2Cl_2 (30 mL) and the corresponding dehydrated (550 °C, overnight) zeolite (1.00 g) for 1 h. After this time, the suspension was filtered and submitted to continuous solid-liquid extraction for 10 h with CH_2Cl_2 as solvent using a micro-Soxhlet equipment. The resulting yellow zeolites were characterized by DR and IR and subsequently reacted with neat anisole (5 mL) at reflux temperature for 30 min. The solids were recovered, washed with CH_2Cl_2 , and thoroughly extracted (CH_2Cl_2) until no more organic material could be observed in the liquid extracts. The combined supernatants were analyzed by GC-MS (Hewlett-Packard 5899A spectrometer). Similar procedures were followed using benzene or toluene instead of anisole. Reactions of xanthone (50 mg) with benzene derivatives (5 mL) in the presence of activated zeolite (1.00 g) were carried out at reflux temperature (5 h) and submitted to exhaustive solid-liquid extraction. Finally all the samples were pump out under 10^{-1} Torr for 2 h.

Test reactions were carried out simultaneously by stirring at 40 °C a solution of α -methylstyrene (40 mg) in CH_2Cl_2 (25 mL) in the presence of the corresponding zeolite (100 mg). The course of the reaction was periodically followed by GC/MS (Fisons MD800 using a 30 m, 5% phenylmethylsilicone capillary column). No significant differences between the original and the zeolites containing AnX^+ could be observed. After 3 h,

the liquid phase was finally analyzed by ^1H NMR (CDCl_3 , 400 MHz Varian spectrometer). Identity of the products was established after chromatographic isolation by comparison of their spectroscopic properties with those previously reported.³⁶

The composites containing 9-arylxanthenium ions were analyzed by combustion chemical analysis using a Fisons EA 1108 CHNS-O elemental analyzer. Thermogravimetric profiles were measured using a Netzsch-STA 409 EP thermobalance under air flow. IR spectra were obtained at room temperature using greaseless quartz cells fitted with CaF_2 windows in a Nicolet spectrophotometer controlled by a work station. Wafers (10 mg) were pressed into disks and outgassed under 10^{-2} Torr at 200 °C for 1 h before to record the spectra. The IR spectrum of unsubstituted X^+ ion in HMor corresponds to the same sample prepared in ref 2. DR spectra were carried out using a Shimadzu UV-2101 PC fitted with an integrating sphere setup and using BaSO_4 as standard.

Fluorescence spectra were recorded using a Perkin-Elmer LS-50 luminescence spectrometer with a front-face attachment for solids. Time-resolved fluorescence and diffuse reflectance measurements were carried out using the third harmonic (355 nm; ≤ 10 ns, ≤ 2 mJ/pulse) from a Surelite Nd:YAG laser as the excitation source. The signals from the monochromator/photomultiplier detection system were captured by a Tektronix Model 2440 transient digitizer and transmitted to a Power-Macintosh that controlled the experiment and provided suitable processing and storage capabilities. The software for data acquisition and instrument control has been developed in the LabView 3.1.1 environment from National Instruments. Fundamentals^{54,55} and details⁵⁶ of similar time-resolved diffuse reflectance laser setup have been reported elsewhere. The samples were contained in cells constructed of 3×7 mm² quartz tubing and purged with nitrogen for 30 min before any laser experiments were conducted.

The time-resolved fluorescence measurements were carried out using a Hamamatsu C-4334 streakscope coupled with a spectrograph and capable of simultaneous spectral and time-resolved data acquisition. Further details of the technique are provided in part 15 in this series of papers. Molecular modeling was performed using Insight II Molecular Modeling package of programs using a Silicon Graphics work station.

Acknowledgment. Financial support by the Natural Sciences and Engineering Research Council of Canada through an operating Grant (J.C.S.) and Spanish DGICYT (HG, Project no PB93-0380) are gratefully acknowledged. M.L.C. also thanks to the Spanish Ministry of Education for a Grant. Rosa Torrero is also thanked for her technical assistance in recording the IR spectra. J.C.S. is the recipient of a Killam Fellowship awarded by the Canada Council.

References and Notes

- (1) Corma, A.; Fornés, V.; García, H.; Miranda, M. A.; Primo, J.; Sabater, M. J. *J. Am. Chem. Soc.* **1994**, *116*, 2276.
- (2) Cozens, F. L.; García, H.; Scaiano, J. C. *Langmuir* **1994**, *10*, 2246.
- (3) Corma, A.; Fornés, V.; García, H.; Miranda, M. A.; Sabater, M. J. *J. Am. Chem. Soc.* **1994**, *116*, 9767.
- (4) Baldoví, M. V.; Cozens, F. L.; Fornés, V.; García, H.; Scaiano, J. C. *Chem. Mater.* **1996**, *8*, 152.
- (5) Baldoví, M. V.; Corma, A.; García, H.; Martí, V. *Tetrahedron Lett.* **1994**, *35*, 9447.
- (6) Breck, D. W. *Zeolite Molecular Sieves: Structure, Chemistry and Use*; John Wiley and Sons: New York, 1974.
- (7) Barrer, R. M. *Zeolites and Clay Minerals as Sorbents and Molecular Sieves*; Academic Press: London, 1978.
- (8) *Introduction to Zeolite Science and Practice*; van Bekkum, H.; Flanigen, E. M.; Jansen, J. C., Eds.; Elsevier: Amsterdam, 1991.
- (9) Davis, M. E. *Acc. Chem. Res.* **1993**, *26*, 111.

- (10) Turro, N. J.; Cheng, C.-C.; Corbin, D. R. *J. Am. Chem. Soc.* **1987**, *109*, 2449.
- (11) Sankararaman, S.; Yoon, K. B.; Yabe, T.; Kochi, J. K. *J. Am. Chem. Soc.* **1991**, *113*, 1419.
- (12) Weiss, R. G.; Ramamurthy, V.; Hammond, G. S. *Acc. Chem. Res.* **1993**, *26*, 530.
- (13) Behrens, P. *Adv. Mater.* **1993**, *5*, 127.
- (14) Beck, J. S.; Vartuli, J. C.; Roth, W. J.; Leonowicz, M. E.; Kresge, C. T.; Schmitt, K. D.; Chu, C. T.-W.; Olson, D. H.; Sheppard, E. W.; McCullen, S. B.; Higgins, J. B.; Schlenker, J. L. *J. Am. Chem. Soc.* **1992**, *114*, 10834.
- (15) Cano, M. L.; Corma, A.; Fornés, V.; García, H.; Miranda, M. A.; Baerlocher, C.; Lengauer, C. *J. Am. Chem. Soc.*, in press.
- (16) Adam, W.; Corma, A.; Miranda, M. A.; Sabater, M.-J.; Sahin, C. *J. Am. Chem. Soc.* **1996**, *118*, 2380.
- (17) Tao, T.; Maciel, G. E. *J. Am. Chem. Soc.* **1995**, *117*, 12889.
- (18) Herron, N.; Stucky, G. D.; Tolman, C. A. *J. Chem. Soc. Commun.* **1986**, 1521.
- (19) Herron, N. *Inorg. Chim. Acta* **1986**, *25*, 4714.
- (20) De Vos, D. E.; Thibault-Starzyk, F.; Jacobs, P. A. *Angew. Chem., Int. Ed. Engl.* **1994**, *33*, 431.
- (21) De Vos, D. E.; Feijen, E. J. P.; Schoonheydt, R. A.; Jacobs, P. A. *J. Am. Chem. Soc.* **1994**, *116*, 4746.
- (22) Johnston, L. J.; Wong, D. F. *J. Phys. Chem.* **1993**, *97*, 1589.
- (23) Yoon, K. B.; Huh, T. J.; Corbin, D. R.; Kochi, J. K. *J. Phys. Chem.* **1993**, *97*, 6492.
- (24) Yoon, K. B. *Chem. Rev.* **1993**, *93*, 321.
- (25) Yoon, K. B.; Kochi, J. K. *J. Am. Chem. Soc.* **1989**, *111*, 1128.
- (26) March, J. *Advanced Organic Chemistry: Reactions, Mechanisms and Structures*, 3rd ed.; John Wiley & Sons: New York, 1993.
- (27) Cano, M. L.; Corma, A.; Fornés, V.; García, H. *J. Phys. Chem.* **1995**, *99*, 4241.
- (28) Chen, F. R.; Fripiat, J. J. *J. Phys. Chem.* **1993**, *97*, 5796.
- (29) Cano, M. L.; Fornés, V.; García, H.; Miranda, M. A.; Pérez-Prieto, J. J. *J. Chem. Soc., Chem. Commun.* **1995**, 2477.
- (30) Behrens, P.; Haak, M. *Angew. Chem., Int. Ed. Engl.* **1993**, *32*, 696.
- (31) Kresge, C. T.; Leonowicz, M. E.; Roth, W. J.; Vartuli, J. C.; Beck, J. S. *Nature* **1992**, *359*, 710.
- (32) Magnoux, P.; Canaff, C.; Machado, F.; Guisnet, M. *J. Catal.* **1992**, *134*, 286.
- (33) Farneth, W. E.; Gorte, R. J. *Chem. Rev.* **1995**, *95*, 615.
- (34) Benito, A.; Corma, A.; García, H.; Primo, J. *Appl. Catal.: A* **1994**, *116*, 127.
- (35) Xu, T.; Haw, J. F. *J. Am. Chem. Soc.* **1994**, *116*, 10188.
- (36) Issakov, J.; Litvin, E.; Minachev, C.; Oehlmann, G.; Scharf, V.; Thome, R.; Tibler, A.; Unger, B. In *Zeolites and Related Microporous Materials: State of the Art*; Elsevier Science: Amsterdam, 1994; Vol. 84C, p 2005.
- (37) Ogata, Y.; Takagi, K.; Ishino, I. *J. Org. Chem.* **1971**, *36*, 3975.
- (38) Armengol, E.; A, C.; Garcia, H.; Primo, J. *Appl. Catal.* **1995**, *126*, 391.
- (39) Gotoh, T.; Yamamoto, M.; Nishijima, Y. *J. Polym. Sci.* **1979**, *17*, 143.
- (40) Irie, M.; Masuhara, H.; Hayashi, K.; Mataga, N. *J. Phys. Chem.* **1974**, *78*, 341.
- (41) Asanuma, T.; Yamamoto, M.; Nishijima, Y. *J. Chem. Soc., Chem. Soc.* **1975**, 608.
- (42) Asanuma, T.; Gotoh, T.; Tsuchida, A.; Yamamoto, M.; Nishijima, Y. *J. Chem. Soc., Chem. Commun.* **1977**, 485.
- (43) It is unlikely for AnX^+ (136.5 \AA^2 molecular area) to be located exclusively on the external surface of the particles ($70 \text{ m}^2/\text{g}$ of external surface). In fact, if AnX^+ would be adsorbed exclusively on the external surface of the zeolite grains, a coverage higher than a monolayer would be required (monolayer area of AnX^+ per g of HY at 3.9% loading: 115.7 m^2).
- (44) Samanta, A.; Gopidas, K. R.; Das, P. K. *Chem. Phys. Lett.* **1990**, *167*, 165.
- (45) Samanta, A.; Gopidas, K. R.; Das, P. K. *Chem. Phys. Lett.* **1993**, *204*, 269.
- (46) Samanta, A.; Gopidas, K. R.; Das, P. R. *J. Phys. Chem.* **1993**, *97*, 1583.
- (47) Valentino, M. R.; Boyd, M. K. *J. Org. Chem.* **1993**, *58*, 5826.
- (48) Das, P. K. *Chem. Rev.* **1993**, *93*, 119.
- (49) Johnston, L. J.; Wong, D. F. *Can. J. Chem.* **1992**, *70*, 280.
- (50) Azarani, A.; Berinstain, A. B.; Johnston, L. J.; Kazanis, S. J. *Photochem. Photobiol. A: Chem.* **1991**, *57*, 175.
- (51) Boyd, M. K.; Lai, H. Y.; Yates, K. *J. Am. Chem. Soc.* **1991**, *113*, 7294.
- (52) Corma, A.; García, H.; Iborra, S.; Primo, J. *J. Catal.* **1989**, *120*, 78.
- (53) Cambolor, M. A.; Mifsud, A.; Pérez-Pariente, J. *Zeolites* **1991**, *11*, 792.
- (54) Bohne, C.; Redmond, R. W.; Scaiano, J. C. In *Photochemistry in Organized and Constrained Media*; Ramamurthy, V., Ed.; VCH: New York, 1991; Chapter 3.
- (55) Wilkinson, F.; Kelly, G. In *Handbook of Organic Photochemistry*; Scaiano, J. C., Ed.; CRC Press: Boca Raton, FL, 1989; Vol. 1, p 293.
- (56) Kelly, G.; Willsher, C. J.; Wilkinson, F.; Netto-Ferreira, J. C.; Olea, A.; Weir, D.; Johnston, L. J.; Scaiano, J. C. *Can. J. Chem.* **1990**, *68*, 812.